ELSEVIER

Biophysical Chemistry 71 (1998) 157–172

Biophysical Chemistry

Effects of metal binding affinity on the chemical and thermal stability of site-directed mutants of rat oncomodulin

Lili Zheng [a], Christopher W.V. Hogue [b], John D. Brennan [a,*]

[a] *Department of Chemistry, Brock University, St. Catharines, Ontario L2S 3A1, Canada*
[b] *Samuel Lunenfeld Research Institute, Mt. Sinai Hospital, 600 University Ave., Toronto, Ontario, M5G 1X5, Canada*

Received 21 October 1997; revised 23 December 1997; accepted 23 December 1997

Abstract

Tryptophan fluorescence was used to study the stability and unfolding behavior of several single tryptophan mutants of the metal-binding protein rat oncomodulin (OM); F102W, Y57W, Y65W and the engineered protein CDOM33 which had the 12 residues of the CD loop replaced with a more potent metal binding site. Both the thermal and the chemical stability were improved upon binding of metal ions with the order apo $< Ca^{2+} < Tb^{3+}$. During thermal denaturation, the transition midpoints (T_{un}) of Y65W was the lowest, followed by Y57W and F102W. The placement of the Trp residue in the F-helix in F102W made the protein slightly more thermostable, although the fluorescence response was readily affected by chemical denaturants, which acted through the disruption of hydrogen bonds at the C-terminal end of the F-helix. Under both thermal and chemical denaturation, the engineered protein showed the highest stability. This indicated that increasing the number of metal ligating oxygens in the binding site, either by using a metal ion with a higher coordinate number (i.e., Tb^{3+}) which binds more carboxylate ligands, or by providing more ligating groups, as in the CDOM33 replacement, produces notable improvements in protein stability.

Keywords: Protein; Tryptophan; Oncomodulin; Fluorescence; Stability

1. Introduction

Structure–stability relationships of proteins have long been of interest since alterations which improve the stability of proteins can have important uses both in commercial and biomedical applications [1,2]. There has been a large amount of work done on the study of protein folding and unfolding to understand the factors which influence the chemical and thermal stability of proteins. A variety of techniques have been used to examine protein folding, unfolding and stability, including nuclear magnetic resonance [3], FTIR [4], circular dichroism [5], absorbance spectroscopy [6] and fluorescence spectroscopy [7]. The folding pathways of certain proteins have been extensively characterized only after using a combination of approaches [8]. Fluorescence techniques are most often used in cases where a specific portion of a protein is being investigated. The technique of site-directed mutagenesis makes it possible to place a fluorescent amino acid at a specific site to provide a probe for investigating the unfolding of a specific

* Corresponding author. Tel.: +1-905-688-5550 (Ext. 4115); fax: +1-905-682-9020; e-mail: jbrennan@chemiris.labs.brocku.ca

0301-4622/98/$19.00
PII S0301-4622(98)00096-9

region of the protein, such as a single domain within a multidomain protein.

There are many factors that can affect protein stability. For example, it has been shown that protein stability can be altered by a single point mutation [9]. For metal-ion-binding proteins, loading of metal ions can also affect stability, as has been recently reported for the Ca^{2+}-binding protein cod III parvalbumin [10,11]. In the present report, we are interested in how variations in metal binding affect the stability of the Ca^{2+}-binding protein rat oncomodulin (OM). Single Trp mutants have been prepared with differing affinities for Ca^{2+} and the protein stability has been examined in the presence of different types of metal ions.

Oncomodulin is a small protein with 108 residues and a molecular weight of 11700 Da, and was originally isolated from rat hepatomas [12] which appear early in the carcinogenic process [13]. Oncomodulin is classified as a parvalbumin-like protein based on its primary structure. The sequences of such proteins possess six stretches of α-helices, lettered A through F. The latter four helices flank two functional metal-ion-binding loops known as the CD- and EF-binding loops [14,15]. Typically, the parvalbumin (PV) CD and EF loops are classified as 'Ca^{2+}/Mg^{2+}' sites since they both exhibit high affinity for Ca^{2+} ($K_d < 10^{-7}$ M) and substantial affinity for Mg^{2+} ($K_d < 10^{-4}$ M) [16]. Even though OM shows a high degree of sequence homology to PV, it displays significantly attenuated affinity for Ca^{2+} and Mg^{2+}. Previous work has suggested that OM possesses a high affinity Ca^{2+}/Mg^{2+} site (EF site, $K_{Ca} \sim 10^{-7}$ M, $K_{Mg} \sim 10^{-4}$ M) and a low affinity Ca^{2+}-specific site (CD site, $K_{Ca} \sim 10^{-6}$ M, $K_{Mg} < 10^{-3}$ M) [17].

Native rat oncomodulin contains no tryptophan and only two tyrosine residues at positions 57 and 65. It has previously been shown that binding of metal ions to different OM mutants can induce specific conformational changes which can be monitored by changes in tyrosine fluorescence [18,19]. It is known that binding of Ca^{2+} causes significant structural changes in the loop region [20–22]. Binding of other metal ions such as Mg^{2+} or Tb^{3+} are also able to induce conformational changes [18,19,21].

Site-specific mutagenesis was used to insert single tryptophan residues to provide fluorescent probes at different locations. Such mutants have previously indicated conformational changes of proteins upon metal ion binding. Here, four mutant oncomodulin proteins with single Trp residues were used to probe the stability of the protein; F102W with a Trp replacing a Phe at position 102 of the F-helix, Y57W with a Trp replacing a Tyr within the CD loop, Y65W with a Trp replacing a Tyr at position 65 in the flanking D-helix of the CD loop, and CDOM33 with a modified CD loop prepared by insertion of a 12 amino acid sequence which has significantly higher affinity for Ca^{2+} than the native CD or EF loop and which has a Trp in position 7 of the binding loop (amino acid position 57) [20].

Both the thermal and chemical stability were examined for apo, Ca^{2+}-loaded and Tb^{3+}-loaded OM mutants by fitting the unfolding curves derived from measurements of Trp fluorescence or Tb^{3+} luminescence [7,10,11]. These studies provide useful information regarding the effects of the different mutations and of binding of different metals on the unfolding behaviour and stability of the protein.

Terbium was chosen for these studies since it is a trivalent cation and thus has a higher order of ligand binding, up to nonadentate. Therefore, it is expected to bind more tightly to the metal binding loops and exert a greater stabilizing effect to the protein structure than calcium. Another advantage of using Tb^{3+} is that changes in terbium luminescence can be used to generate unfolding curves. Terbium luminescence upon binding to an EF hand loop can be enhanced by energy transfer (ET) from a nearby fluorescent donor, in this case an aromatic amino acid [23,24]. For single Trp proteins, excitation at a wavelength of 295 nm can be used to exclusively excite tryptophan residues and thus rule out energy transfer processes involving Phe and Tyr. Excitation of tryptophan can then exclusively lead to the transfer of energy to a nearby Tb^{3+}, followed by luminescence of Tb^{3+} resulting from transitions between the $^5D_4$ and $^7F_5$ states (545 nm) and the $^5D_4$ and $^7F_6$ states (490 nm). For Y57W and CDOM33 the Trp residue is directly in the loop region, thus signals from both Trp and Tb^{3+} can be used to follow the effects of global unfolding on the loop region. On the other hand, the Trp residue within Y65W and F102W is outside the loop region, and thus signals resulting from Tyr-57 to Tb^{3+} energy transfer (using excitation at 285 nm)

can be utilized to determine if the unfolding of the loop region (probed by Tb^{3+} luminescence) occurs at the same time as unfolding of the D-helix or F-helix (probed by Trp fluorescence). These studies are used to determine if the unfolding curves derived from fluorescence measurements accurately reflect the global unfolding of the protein.

2. Experimental

2.1. Chemicals

All protein samples were donated by Dr. A.G. Szabo and were used without further purification. Details of the preparation and purification procedures have been described elsewhere [25]. Piperazine-*N*,*N*′-bis[2-ethanesulfonic acid] (PIPES), acrylamide (99 + %) and terbium chloride were supplied by Aldrich (Milwaukee, WS). Ethylenebis(oxyethylenenitrilo)tetraacetic acid (EGTA) and calcium chloride were supplied by Fisher scientific (Toronto, ON). The guanidine hydrochloride (GdHCl, Sequanol grade) was from Pierce (Rockford, IL). The Sephadex G-25 fine powder was supplied by Pharmacia Biotech (Uppsala, Sweden). All water was twice distilled and deionized to a specific resistance of at least 18 MΩ cm using a Milli-Q 5 stage water purification system. All other chemicals were of analytical grade and were used without further purification.

2.2. Procedures

2.2.1. Sample preparation

All proteins were dissolved in 10 mM PIPES buffer containing 100 mM KCl at pH 6.5. Apo proteins were prepared by addition of a 350-fold excess of EGTA as determined by EGTA titration curves of proteins containing either Ca^{2+} or Tb^{3+}. Metal loaded proteins were prepared by adding a 50-fold excess of Ca^{2+} or a 3-fold excess of Tb^{3+} to the proteins. The concentration of protein was determined by UV–Vis absorbance measurements using $\epsilon_{280} = 6900\ M^{-1}\ cm^{-1}$ for Y57W, Y65W and CDOM33, and $\epsilon_{280} = 8200\ M^{-1}\ cm^{-1}$ for F102W [18–22]. Terbium-loaded samples were prepared as follows. A 100 μM $TbCl_3$ solution was prepared in PIPES buffer and the exact concentration of the Tb^{3+} solution was determined by a dipicolinic acid titration [26]. A volume of 2 ml of protein with a concentration of 2 μM was titrated with the Tb^{3+} solution to reach a 3:1 molar ratio of terbium to protein.

2.2.2. Fluorescence spectra

Fluorescence spectra were collected using instrumentation which is described elsewhere [27]. The concentration of protein was 4 μM for apo experiments and 2 μM for other experiments. Samples were excited at 295 nm and emission was collected from 305 nm to 450 nm for Ca^{2+}-free and for Ca^{2+}-loaded proteins and from 305 nm to 570 nm for Tb^{3+}-loaded proteins. All spectra were collected in 1 nm increments at a rate of 180 nm min^{-1} and with an integration time of 0.30 s. Samples were continuously stirred throughout the experiments and were maintained at a temperature of 20 ± 0.2°C (except where otherwise stated) using a Neslab R110 recirculating water bath. Appropriate blanks were subtracted from each sample and the spectra were corrected for deviations in emission monochromator throughput and PMT response. Spectra were integrated from the emission maximum to the red end of the spectra to avoid scattering contributions at the blue end of the spectra.

2.2.3. EGTA titrations

A volume of 1700 μl of a solution containing 4 μM protein in the presence of a 50-fold excess of Ca^{2+} or a 3-fold excess of Tb^{3+} was placed into a quartz cuvette. Aliquots of 50 mM EGTA were added with constant stirring to reach a ratio of EGTA versus protein of 350 to 1. A fluorescence spectrum was taken at each point for both a sample and a blank containing the same amount of EGTA to follow the removal of the metal ions from the different proteins.

2.2.4. Chemical denaturation studies

A volume of 1.75 ml of the protein solution was added to a quartz cuvette. A total of twenty aliquots of 8.0 M GdHCl in buffer were added with constant stirring and a minimum of 5 min was allowed for equilibration after each addition. A fluorescence

spectrum was collected at each point for both the sample and a blank containing an identical concentration of GdHCl. The spectra were corrected for dilution factors and integrated from the emission maximum to the red end of the spectra. The integrated intensity was normalized to the initial intensity and was plotted against denaturant concentration to generate the unfolding curve.

Unfolding transitions were fitted using the equation given by Santoro and Bolen [28]:

$$F_D = \frac{(F_N + m_N[D]) + (F_U + m_U[D])\exp\{-\Delta G_{un}/RT + m_G[D]/RT\}}{1 + \exp[-\Delta G_{un}/RT + m_G[D]/RT]} \quad (1)$$

where F_D is the value of the fluorescence intensity at a given concentration of denaturant, $[D]$, R is the gas constant and T is the temperature. The remaining six terms are fitting parameters, where F_N and F_U are the values of the intensity extrapolated to zero concentration of denaturant for the native and unfolded states, respectively, m_N and m_U are the slopes for the dependencies of F_N and F_U on denaturant concentration, ΔG_{un} is the free energy of unfolding, and m_G is the denaturant index describing the dependence of ΔG_{un} on denaturant concentration. The transition midpoint $(C_{1/2})$ values were calculated by dividing ΔG_{un} by $-m_G$. The reversibility of unfolding was determined by measuring the spectra after dialyzing denatured protein against fresh buffer and running the denatured protein through a Sephadex G-25 column.

2.2.5. Thermal denaturation studies

It was found that careful removal of oxygen before each experiment was required to prevent protein aggregation. Removal of oxygen was performed by purging nitrogen through the buffer before diluting the stock solution. In addition, the air space of the cuvette was also filled with nitrogen. In the absence of nitrogen purging, aggregation of protein was observed to decrease the thermal stability as well as decrease the percent signal recovery upon cooling the sample to room temperature.

A volume of 1.0 ml of the protein solution was placed into a quartz fluorimeter cuvette. The cuvette was properly sealed to avoid concentration changes which could be caused by evaporation of buffer solution at high temperatures. The temperature was raised in ca. 5°C increments starting at 20°C and going to 95°C, then lowered to 20°C to check reversibility. A fluorescence spectrum was collected from the sample and from an appropriate 'no protein' blank at each temperature. The temperature of the solution in a second cuvette which was also present in the 4 sample turret was measured directly using a thermistor probe (Hanna Instruments model 9043A) to account for loss of heat through the tygon tubing connecting the sample holder and the water bath. The samples were allowed to equilibrate for at least five minutes at each temperature before readings were taken. Spectra were integrated from the emission maximum to the red end of the spectra. The integrated intensity was normalized to the intensity at the starting temperature (usually 20°C) and was plotted against temperature to generate the unfolding curve. The unfolding curves were corrected for contributions from thermally induced quenching using standard methods [7]. In many cases, this resulted in non-sloping initial and final portions to the curve [29], as expected for a thermally induced unfolding of a protein.

The unfolding enthalpy change (ΔH^0_{un}) and entropy change (ΔS^0_{un}) were calculated by fitting the unfolding curve to the following equation [7]:

$$F_T = \frac{(F_{0N} + s_N T) + (F_{0U} + s_U T)\exp\{-\Delta H^0_{un}/RT + \Delta S^0_{un} T/RT\}}{1 + \exp[-(\Delta H^0_{un}/RT + \Delta S^0_{un} T/RT)]} \quad (2)$$

where F_T is the fluorescence at a given temperature T, F_{0N} and F_{0U} are the fluorescence intensity of the native state and unfolded state at a given reference temperature (20°C), s_N and s_U are the temperature dependence of the fluorescence of the native and denatured state and R is the gas constant. The transition temperature (T_{un}) was calculated by dividing ΔH^0_{un} by ΔS^0_{un}. The free energy change for unfolding (ΔG_{un}) was determined by using Eq. (2), with a reference temperature (T_r) of 20°C

$$\Delta G_{un}(T_r) = \Delta H^0_{un} - T_r \Delta S^0_{un} + \Delta C_{p,un} \times [(T_r - T_{un}) - T_r \ln(T_r/T_{un})] \quad (3)$$

where $\Delta C_{p,un}$ is differential heat capacity for unfolding, and accounts for the temperature sensitivity of the entropy and enthalpy terms on going from T_r to T_{un}.

2.2.6. Acrylamide quenching studies

2.0 ml of a 2 μM protein solution was titrated by adding a total of twenty-two 10 μL aliquots of 8.0 M acrylamide in buffer. A fluorescence spectrum was collected from the sample and an appropriate blank after each addition. Spectra were corrected for sample dilution and were integrated as described above. The data were analyzed using a modified version of the Stern–Volmer (SV) equation which accounts for both dynamic and static quenching of Trp fluorescence [30a,30b] as given in Eq. (4):

$$\frac{F_0}{Fe^{V[Q]}} = 1 + K_{SV}[Q] = 1 + k_q\tau_0[Q] \quad (4)$$

where F_0 is the fluorescence intensity in the absence of the quencher, F is the fluorescence intensity at a given molar concentration of quencher $[Q]$, K_{SV} is the Stern–Volmer quenching constant (M^{-1}), k_q is the bimolecular quenching constant (M^{-1} ns^{-1}), τ_0 is the unquenched fluorescence lifetime (ns) and V represents the volume (in M^{-1}) of the active quenching sphere within which the quenching of the fluorophore is instantaneous. To calculate k_q values, mean lifetime values for apo and holo proteins were obtained from the literature [19–21]. Mean lifetime values for denatured proteins were obtained by the time-correlated single photon counting method using instrumentation and fitting procedures which are described in detail elsewhere [31a,31b]. The decays were assumed to be a sum of discrete exponential decay components, and all decays were fit to a sum of three decay components.

3. Results and discussion

3.1. Fluorescence properties of native oncomodulin mutants

The fluorescence properties of the native proteins in the presence and absence of Ca^{2+} and Tb^{3+} are shown in Table 1 along with the changes in the spectral properties and quantum yield values resulting from chemical denaturation. Initial studies focused on apo proteins which were prepared by addition of the chelating agent EGTA. To test the effectiveness of this method, each protein was loaded with a 3-fold excess of Tb^{3+} (which binds more strongly to OM than does Ca^{2+}) and the emission of

Table 1
Changes in fluorescence properties for apo, Ca^{2+}-loaded and Tb^{3+}-loaded oncomodulin mutants during chemical denaturation

Protein	$\Phi_{(native)}$	$\Phi_{(denatured)}$	Change of λ_{max} (nm)	Change of FWHM (nm)
Y57W				
Ca^{2+}-free	0.133[a]	0.095	341–337–345[b]	55–58
Ca^{2+}-loaded	0.078	0.101	339–345	54–58
Tb^{3+}-loaded	0.027	0.106	339–345	54–58
Y65W				
Ca^{2+}-free	0.143	0.105	343–346	55–57
Ca^{2+}-loaded	0.157	0.126	343–345	56–57
Tb^{3+}-loaded	0.156	0.113	343–345	56–57
F102W				
Ca^{2+}-free	0.190	0.087	317–345	47–64
Ca^{2+}-loaded	0.240	0.070	315–345	39–64
Tb^{3+}-loaded	0.212	0.082	315–345	39–64
CDOM33				
Ca^{2+}-free	0.101	0.109	340–345	55–57
Ca^{2+}-loaded	0.152	0.097	339–345	55–58
Tb^{3+}-loaded	0.023	0.058	339–345	55–58

[a] Errors in Φ values are ± 0.001 in all cases.
[b] In this case, the wavelength first blue-shifted, then red-shifted.

the Tb^{3+} peak at 545 nm was monitored as EGTA was added. In all cases, the Tb^{3+} emission peak was completely eliminated upon addition of a 350-fold excess of EGTA, indicated that the proteins were apo under these conditions. The similarity of our spectral data for the apo proteins (shown in Table 1) to that of Szabo and co-workers [18–22] (who used trichloroacetic acid precipitation for decalcification of proteins) indicates that the use of EGTA for preparation of apo proteins is an acceptable method. Thus, all studies of apo proteins reported herein were done with a 350-fold excess of EGTA present.

The fluorescence characteristics of the holo proteins were substantially different than those of the apo proteins. Binding of Ca^{2+} generally caused only small blue-shifts in wavelength (1–2 nm) as was observed by Hutnik et al. [19,21]. However, the changes in intensity upon binding of Ca^{2+} were significant, as shown by the fluorescence quantum yields reported in Table 1. For F102W, binding of Ca^{2+} caused the emission intensity to increase by ca. 30% with no significant changes in the shape or position of the spectrum. These finding are consistent with those of Hutnik et al. [21]. The emission maximum and full-width-at-half-maximum (FWHM) values for the holo-F102W mutant suggested that the Trp was in a hydrophobic region which was shielded from solvent. This is consistent with the position of the F-helix from X-ray diffraction data [32]. Acrylamide quenching results, shown in Table 2, also support this suggestion. K_{SV} values were measured and were used to obtain bimolecular quenching constants using fluorescence lifetime data which was reported elsewhere [18–22]. The fluorescence decays of most mutants showed two or three components and thus intensity-weighted mean lifetimes were calculated (using the equation provided in the footnotes in Table 2) to obtain the k_q values. The acrylamide quenching results showed that the environment of the Trp residue in F102W became significantly less exposed upon addition of Ca^{2+}, with the k_q value decreasing by 35%.

In the case of Y65W there was only very small increase in intensity ($\sim 5\%$) and no shift in the emission maximum upon binding of Ca^{2+}. This small intensity change indicated that the environment around Trp at position 65 did not change significantly upon addition of calcium. This is supported by the small change ($< 10\%$) in the k_q value on going from the apo to the holo form of the protein.

Table 2
Stern–Volmer quenching constants and bimolecular quenching rate constants from acrylamide quenching of oncomodulin mutants

Protein	V (M^{-1})	K_{sv} (M^{-1})	$\langle\tau\rangle$ (ns)[a]	k_q (M^{-1} ns^{-1})
Y57W				
apo	0.8[b]	8.69 ± 0.08	2.43 ± 0.01[c]	3.58 ± 0.03
holo	0.8	4.66 ± 0.04	1.83 ± 0.02[c]	2.55 ± 0.02
denatured	1.0	8.13 ± 0.06	2.96 ± 0.01[f]	2.75 ± 0.03
Y65W				
apo	1.2	7.03 ± 0.06	2.29 ± 0.02[c]	3.07 ± 0.03
holo	0.9	6.39 ± 0.04	2.33 ± 0.01[c]	2.74 ± 0.03
denatured	1.5	7.48 ± 0.06	3.41 ± 0.01[g]	2.19 ± 0.02
F102W				
apo	1.0	5.00 ± 0.04	3.12 ± 0.02[d]	1.60 ± 0.02
holo	0.2	3.98 ± 0.03	3.80 ± 0.02[d]	1.05 ± 0.01
denatured	2.4	9.25 ± 0.08	2.93 ± 0.02[h]	3.16 ± 0.03
CDOM33				
apo	1.0	7.33 ± 0.07	2.65 ± 0.02[e]	2.77 ± 0.03
holo	0.8	7.83 ± 0.07	2.53 ± 0.02[e]	3.09 ± 0.03
denatured	1.1	7.23 ± 0.07	2.89 ± 0.02[i]	2.50 ± 0.02

[a] Intensity-weighted mean lifetime values were calculated using $\langle\tau\rangle = \Sigma(\alpha_i\tau_i^2)/\Sigma(\alpha_i\tau_i)$.
[b] All V values have errors of ± 0.1 M^{-1}.
[c] From Ref. [19].
[d] From Ref. [21].
[e] From Ref. [20].
[f] $\alpha_1 = 0.24$, $\alpha_2 = 0.49$, $\alpha_3 = 0.27$, $\tau_1 = 4.132$ ns, $\tau_2 = 1.893$ ns $\tau_3 = 0.283$ ns, SVR = 1.98, $\chi^2 = 1.048$.
[g] $\alpha_1 = 0.30$, $\alpha_2 = 0.44$, $\alpha_3 = 0.26$, $\tau_1 = 4.507$ ns, $\tau_2 = 1.968$ ns $\tau_3 = 0.308$ ns, SVR = 1.91, $\chi^2 = 0.997$.
[h] $\alpha_1 = 0.22$, $\alpha_2 = 0.35$, $\alpha_3 = 0.43$, $\tau_1 = 3.801$ ns, $\tau_2 = 1.303$ ns $\tau_3 = 0.147$ ns, SVR = 1.88, $\chi^2 = 1.023$.
[i] $\alpha_1 = 0.27$, $\alpha_2 = 0.47$, $\alpha_3 = 0.26$, $\tau_1 = 4.316$ ns, $\tau_2 = 1.961$ ns $\tau_3 = 0.264$ ns, SVR = 2.01, $\chi^2 = 1.000$.

Inspection of the quantum yield and k_q values for apo Y57W and CDOM33 indicated that the Trp residue was likely in a somewhat different environment for each protein, with the Trp residue of Y57W being more solvent exposed than that of CDOM33, even though the quantum yield of Y57W was higher than that of CDOM33. Addition of Ca^{2+} caused the local environment of the Trp residue to change dramatically for both proteins, with an enhancement in the quantum yield of Trp within CDOM33, but a significant quenching of intensity for Y57W. Over-

all, the intensity of CDOM33 increased by 40% while the intensity of Y57W decreased by 40% upon binding of Ca^{2+}.

The k_q values also showed that the environment of Trp in Y57W and CDOM33 was significantly different upon binding of Ca^{2+}. However, the k_q value of Y57W unexpectedly decreased from 3.58 to 2.55 M^{-1} ns^{-1} while the k_q value for CDOM33 increased from 2.77 to 3.05 M^{-1} ns^{-1} upon binding of Ca^{2+}. These results clearly show that the Trp at position 57 in Y57W became less exposed on addition of calcium, while that in CDOM33 became more exposed, indicating significantly different structural responses to the addition of calcium. Interestingly, the changes in exposure to solvent are opposite to those expected from the changes in quantum yield. Generally, greater exposure of a Trp residue to solvent results in an increase in collisional quenching, producing a decrease in the quantum yield. The apparent inconsistency between the k_q and quantum yield values can be resolved by recognizing that the addition of Ca^{2+} will dramatically alter the electrostatic environment in the region of Trp-57. It has previously been reported that the relative change in fluorescence lifetime for Y57W upon binding of Ca^{2+} does not correspond to the relative change in quantum yield, even though there is no evidence for static quenching of the Trp at position 57. The assertion has been made that the binding of Ca^{2+} can result in substantial changes in the radiative lifetime (τ_R) of the Trp residue (note: $\tau_R = \tau_S/\Phi$ where the singlet state lifetime (τ_S) is given by $\tau_S = \Sigma\alpha_i\tau_i$) [19,33]. Our calculations show that the binding of Ca^{2+} to Y57W resulted in an increase in the radiative lifetime from 18.3 to 23.4 ns (using the data in Ref. [19]), while binding of Ca^{2+} to CDOM33 produced a decrease of k_R from 26.5 ns to 16.9 ns. This strongly suggests that the conformational changes in the loop region upon binding of Ca^{2+} are substantially different for the two mutants.

Binding of terbium to oncomodulin mutants caused substantial quenching of Trp fluorescence and a large increase in terbium luminescence for both CDOM33 and Y57W when compared to the holo-forms. This is consistent with the short Trp-to-Tb^{3+} donor–acceptor distance for CDOM33 and Y57W (ca. 4.5 and 8.0 Å from the CD and EF loops, respectively [19]). On the other hand, there were only small changes in the emission intensity of the Trp residue in F102W and Y65W, suggesting that energy transfer to Tb^{3+} was not efficient for these proteins. From the crystal structure of wild-type OM, the gamma-carbon of F-helix Phe 102 is 10.8 Å away from the nearest calcium in the EF loop [31a,31b], while the gamma-carbon of the D-helix Tyr-65 is 11.4 Å away from the CD loop calcium. Hence, the Trp residue within these proteins is not within the required distance for efficient energy transfer by the electron exchange mechanism [23,24].

3.2. Chemical denaturation of apo proteins

Initial studies concentrated on the stability of apo proteins. The unfolding curves are shown in Fig. 1. Several aspects of these curves merit special attention. First, the intensity of both F102W and Y65W decreased immediately upon addition of denaturant, resulting in the absence of a pre-unfolding baseline. In both cases, both the intensity and wavelength data indicated that the unfolding process was completed at a relatively low GdHCl concentration. Second, the unfolding profiles of Y57W and CDOM33 showed opposite intensity trends on unfolding. The intensity of Y57W decreased by about 30% with an initial blue shift of 4–5 nm in the emission maximum followed by a red-shift to the characteristic emission

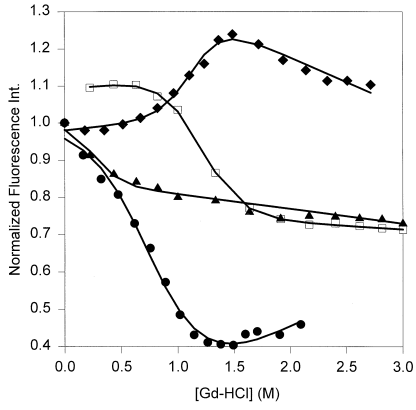

Fig. 1. Fluorescence intensity changes as a function of GdHCl concentration for calcium-free, F102W (●), Y65W (▲), Y57W (□) and CDOM33 (♦). The symbols are the experimentally derived data points. The solid lines are the lines-of-best-fit as determined by fitting to Eq. (1). Fitting parameters are given in Table 3.

maximum of 345 nm which is indicative of a fully exposed Trp residue. The intensity of CDOM33, on the other hand, increased by approximately 20% followed by a decrease of 10% during the addition of GdHCl. The transition between 1.0 and 1.5 M of GdHCl showed a red-shift in the emission maximum which corresponded to the initial increase of intensity. Finally, the final quantum yield values for the Y57W and CDOM33 suggested similar environments for the exposed Trp residue in the two proteins.

The reversibility of the chemically induced unfolding was tested for all oncomodulin mutants by dialyzing the denatured protein against fresh buffer and then running denatured proteins through a Sephadex G-25 column. The spectra reversed fully and the refolded proteins showed similar binding behavior to the native protein. This indicated that thermodynamic analysis of the unfolding curves generated by chemical denaturation could be done.

The unfolding free energies and transition midpoints for each apo protein were obtained by fitting the integrated intensity data. In the case of the Y57W mutant, the initial rise in intensity upon the first addition of denaturant made it impossible to fit the baseline region if the initial point was included. For this reason, the fitting was done starting at the second point in the titration. This has the effect of shifting the entire unfolding curve upward, and affects that values of s_N and F_{0N} in Eq. (1). However, this fitting procedure has no affect on the values of m_G, ΔG_{un}, or $C_{1/2}$ since these values depend on slopes, and thus are not affected by shifting the curve in the *y*-direction. In fitting the unfolding curves, it was assumed that the unfolding transitions followed a two-state model. Our unfolding curves clearly indicated two-state unfolding processes for the various proteins, indicating that this assumption was valid. We also assumed that the Trp fluorescence reported on changes in the global structure of the protein. The validity of the assumption is described further in Section 3.4.

The fitting results for all apo proteins are shown in Table 3. The ΔG_{un} and $C_{1/2}$ values of Y57W and CDOM33 were quite similar suggesting that there was not a significant difference in the chemical stability of the protein when the modified CD loop was present but had no metal ions bound. The free energy and transition midpoint values for F102W were significantly lower than for the proteins with the Trp present in the loop region. This may indicate that the presence of the Trp residue at position 102 slightly destabilized the apo protein. Y65W had the lowest free energy and transition midpoint among these mutants (about 1.0 kcal mol^{-1} and 0.37 M lower than F102W). Position 65 is interesting in that it is a kink point in the D-helix. The kink in this

Table 3
Free energy changes for chemical unfolding of oncomodulin obtained by fitting of unfolding curves to Eq. (1)

Proteins	ΔG_{un} (kcal mol^{-1})	m_G (kcal l mol^{-2})	$C_{1/2}$ (M)
Ca^{2+}-free[a]			
Y57W	3.9 ± 0.3	3.2 ± 0.2	1.2 ± 0.1
Y65W	0.6 ± 0.1	1.9 ± 0.4	0.3 ± 0.1
F102W	1.9 ± 0.1	2.2 ± 0.2	0.8 ± 0.1
CDOM33	3.0 ± 0.3	2.7 ± 0.3	1.2 ± 0.1
Ca^{2+}-loaded[b]			
Y57W[d]	6.7 ± 0.5	3.3 ± 0.3	2.0 ± 0.1
Y65W	6.6 ± 0.5	3.4 ± 0.3	1.9 ± 0.1
F102W	5.2 ± 0.5	2.9 ± 0.3	1.8 ± 0.1
CDOM33	6.9 ± 0.4	3.1 ± 0.2	2.2 ± 0.1
Tb^{3+}-loaded[c]			
Y57W[e]	7.8 ± 0.5	2.8 ± 0.2	2.8 ± 0.1
Y65W	6.7 ± 0.7	2.3 ± 0.3	2.9 ± 0.1
F102W	8.0 ± 0.8	3.1 ± 0.3	2.6 ± 0.2
F102W[c]	11.1 ± 1.5	4.2 ± 0.5	2.6 ± 0.3
CDOM33[c]	8.5 ± 0.9	2.1 ± 0.2	4.0 ± 0.1

[a] Fitting parameters for apo proteins were as follows: F102W: $F_N = 1.00$, $F_U = 0.137$, $m_N = 0.00$, $m_U = 0.157$; Y65W: $F_N = 1.00$, $F_U = 0.848$, $m_N = 0.00$, $m_U = -0.039$; Y57W: $F_N = 1.091$, $F_U = 0.768$, $m_N = 0.037$, $m_U = 0.108$; CDOM33: $F_N = 0.980$, $F_U = 1.444$, $m_N = 0.030$, $m_U = 0.133$.

[b] Fitting parameters for Ca^{2+}-loaded proteins were as follows: F102W: $F_N = 1.010$, $F_U = 0.260$, $m_N = 0.121$, $m_U = 0.023$; Y65W: $F_N = 0.982$, $F_U = 0.745$, $m_N = 0.016$, $m_U = -0.016$; Y57W: $F_N = 339$, $F_U = 345$, $m_N = 0.00$, $m_U = 0.00$; CDOM33: $F_N = 1.042$, $F_U = 0.772$, $m_N = 0.00$, $m_U = -0.013$.

[c] Fitting parameters for Tb^{3+}-loaded proteins were as follows: F102W (Trp): $F_N = 1.009$, $F_U = 0.357$, $m_N = -0.112$, $m_U = -0.002$; F102W (Tb^{3+}): $F_N = 0.994$, $F_U = 0.273$, $m_N = -0.172$, $m_U = -0.008$; Y65W: $F_N = 0.995$, $F_U = 0.316$, $m_N = 0.021$, $m_U = 0.056$; Y57W: $F_N = 0.996$, $F_U = 0.377$, $m_N = 0.016$, $m_U = -0.021$; CDOM33: $F_N = 1.031$, $F_U = 0.261$, $m_N = 0.032$, $m_U = -0.006$.

[d] The thermodynamic parameters were obtained by fitting emission maxima data.

[e] The thermodynamic parameters were obtained by fitting Tb^{3+} luminescence data.

helix seems necessary to allow the D-helix to wrap tightly around the hydrophobic core of the protein. It appears that the apo protein is significantly affected by the insertion of a Trp at position 65, resulting in the low local free energy of unfolding when the Trp is at position 65.

3.3. Chemical denaturation of holo (Ca^{2+}-loaded) proteins

Loading of Ca^{2+} caused substantial changes in the unfolding behaviour and the overall stability of the various oncomodulin mutants. The unfolding curves are shown in Fig. 2, while the changes in the spectroscopic parameters upon denaturation are shown in Table 1. Denaturation of each of the holo proteins caused a typical red-shift in the emission maximum (λ_{max}) and a change in fluorescence intensity as summarized in Table 1. F102W OM showed the greatest change in both quantum yield (75% decrease) and emission maximum (30 nm increase). The FWHM of this protein also increased by 25 nm upon unfolding. The intensity of F102W started to decrease immediately upon addition of denaturant; however, the main unfolding transition reported by both the intensity and emission maximum value did not begin until 1.0 M GdHCl was present. These results suggested that the interaction of GdHCl with the protein may have caused the protein structure to be loosened and the quantum yield to decrease before the main unfolding process had begun.

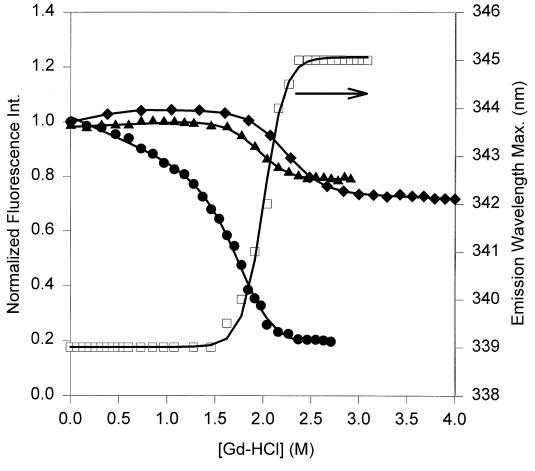

Fig. 2. Fluorescence intensity changes as a function of GdHCl concentration for calcium-loaded F102W (●), Y65W (▲), Y57W (□) and CDOM33 (♦). The symbols are the experimentally derived data points. The solid lines are the lines-of-best-fit as determined by fitting to Eq. (1). Fitting parameters are given in Table 3.

This explanation is also supported by acrylamide quenching experiments which were done at different GdHCl concentrations. The active quenching sphere V (from Eq. (4)) increased by 0.8 M^{-1} when the concentration of GdHCl increased from 0 to 1.6 M; however, the values of the Stern–Volmer constant (K_{SV}) stayed relatively constant (4.0–5.0 M^{-1}). There was a large increase in both the V and K_{SV} values when the concentration of GdHCl exceeded 1.9 M, at which point the main unfolding process began. The completely unfolded protein had a V value of 2.4 M^{-1} and a K_{SV} value of 9.25 M^{-1} at 2.55 M GdHCl, indicative of a fully exposed Trp residue [34]. In addition, the k_q value increased by 3-fold compared to the value of the native holo protein, again indicating that the Trp was fully exposed.

The unfolding curve of Y65W showed an intensity and wavelength profile which matched closely. Both the intensity and the wavelength values showed a narrow transition range (1.6–2.5 M GdHCl). Overall, the quantum yield of Y65W decreased by about 20% upon unfolding, while the emission maximum red-shifted by 4 nm. These changes corresponded to a slight increase in the exposure of the Trp residue (as determined by the V and k_q values shown in Table 2).

CDOM33 and Y57W OM showed similar changes in the emission maximum (9 nm) and FWHM values (3–4 nm) upon unfolding. However, the intensity profiles of these two proteins were remarkably different. Overall, CDOM33 had a decrease of 35% in intensity during denaturation while the intensity of Y57W increased by 30% upon unfolding (see Table 1). The quantum yield of the two proteins were identical (within error), suggesting that the proteins were completely unfolded. This suggestion is supported by the reasonable similarity in the k_q and V values for the unfolded proteins (Table 2). The similarity in the quantum yields and k_q values strongly suggests that adjacent residues were not acting as static quenchers of fluorescence, in agreement with previous reports [19]. The observed increase in the

fluorescence intensity upon denaturation of Y57W is intriguing. It is apparent that the unfolding process, which generally causes a decrease in intensity, was competing with the decalcification process, which causes a 70% increase in intensity for Y57W. The combined effects of these processes resulted in an overall increase in intensity of 30% for the unfolding process.

The unfolding energies and transition midpoints for each of the proteins were obtained by fitting the intensity data to Eq. (1). The results are shown in Table 3. Owing to the combination of processes which affected the intensity of Y57W, the unfolding of this protein could not be adequately fit using intensity data. Therefore, changes in the emission wavelength during unfolding were used in this case. This approach is valid when the quantum yield does not change significantly between the folded and unfolded forms (this being one reason why fits to intensity-based data were problematic). To check this assumption, both intensity and emission maximum data were used to calculate thermodynamic parameters for CDOM33, which underwent similar intensity changes when compared to Y57W. Similar thermodynamic data was obtained in both cases.

The most obvious difference between the holo and apo proteins is that the stability of each protein increased substantially upon binding of Ca^{2+}, indicating that the metal ions preferentially bind to the folded form of the protein. However, not all proteins were stabilized to the same degree. For example, the stabilization, or $\Delta(\Delta G_{un})$ value, on going from the apo to the holo form of Y57W (2.9 kcal mol^{-1}), F102W (3.3 kcal mol^{-1}) or CDOM33 (3.9 kcal mol^{-1}) was substantially lower than that for Y65W (6.0 kcal mol^{-1}). Hence, we observe that Ca^{2+} binding can overcome the destabilizing effects of inserting a Trp into position 65 of the D-helix. The F102W mutant was stabilized to a similar degree when compared to Y57W or CDOM33, but still had the lowest unfolding free energy and transition midpoint. Thus even for the Ca^{2+}-loaded form, the insertion of the Trp into the F-helix still results in partial destabilization of the protein.

CDOM33 was observed to have the highest free energy and transition midpoint (2.2 M). Since the whole CD loop was modified for CDOM33 to provide higher binding affinity [20], the higher free energy and higher transition midpoint were not unexpected. This result proved that increases in the binding affinity can stabilize the native structure of the holo-protein. Altering of binding affinity can be achieved by either replacing the loop with residues which can provide a higher binding affinity or by loading the protein with other metal ions which have higher binding affinity.

3.4. Chemical denaturation of Tb^{3+}-loaded proteins

To further explore the effects of metal ions on protein stability, unfolding experiments were done for proteins containing a 3:1 molar ratio of Tb^{3+}:protein. It is important to note that the concentration of Tb^{3+} used in this part of the study was significantly less than that used for the study of Ca^{2+}-loaded proteins (50:1 Ca^{2+}:protein). In general, the stability of a ligand binding protein will depend on the concentration of ligand [10,11], and hence the thermodynamic parameters determined in this work will depend on metal ion concentration. However, the purpose of this study was not to examine protein stability as a function of metal ion concentration, but rather as a function of binding affinity. The choice of metal ion concentration was determined by the level at which maximum stability was obtained. For Ca^{2+}, maximum stability occurred at a concentration of metal ion which was 50-fold higher that the protein concentration. For Tb^{3+}, the addition of a 50-fold excess of the metal ion resulted in aggregation of the protein, and thus could not be used. Instead, the level for maximum stability (in this case a 3:1 Tb^{3+}:protein ratio) was used.

The terbium luminescence peaks at 545 nm and 490 nm resulting from ET from nearby Trp residues can be used to provide additional signals which can be utilized to monitor the unfolding process. According to the ranking of calcium binding proteins by terbium sensitivity obtained by Hogue et al. [23], when excited at 285 nm, the terbium signal ratio of CDOM33:Y57W:Y65W:F102W is 30:6:4:1. At an excitation wavelength of 295 nm, the sensitivity of the Tb^{3+} luminescence enhancement for Y65W and F102W is further decreased since energy transfer contributed from Tyr 57 is removed. However even at 295 nm excitation it is still possible to utilize the Tb^{3+} peaks as a secondary signal to monitor the

unfolding process of proteins. In the case of Y57W and CDOM33 the Trp residue is located within the binding loop, resulting in very efficient energy transfer from Trp to Tb^{3+}. Therefore, for these proteins the terbium peak was used as a primary signal while the Trp peak was used as a secondary signal. The use of Tb^{3+} or Trp luminescence is noted in the figure captions.

The unfolding curves of the Tb^{3+} loaded proteins is shown in Fig. 3. It was noticed that in some cases the curves originally appeared to show 2 unfolding steps. However, it was determined that the initial decrease in intensity was the result of dissolution of aggregates which had formed during storage of Tb^{3+} loaded proteins. Titrations on freshly prepared samples always showed a single transition, indicative of a 2-step unfolding process. The free energy and transition midpoint values are shown in Table 3. It was necessary to use Tb^{3+} luminescence data to fit the unfolding transitions of Y57W and CDOM33 since the intensity of the Trp residue was affected by both changes in energy transfer to Tb^{3+} and exposure of Trp to solvent upon protein unfolding, resulting in non-linear baseline regions. The unfolding of Y65W was fit using changes in Trp intensity upon unfolding, while both the Trp signal originating from position 102 (excitation at 295 nm) and the Tb^{3+} signal resulting from energy transfer from Try-57 (excitation at 285 nm) were measured during chemical denaturation of the F102W mutant. This last experiment was done to examine the key question of whether Trp fluorescence reported on local or global unfolding of the protein.

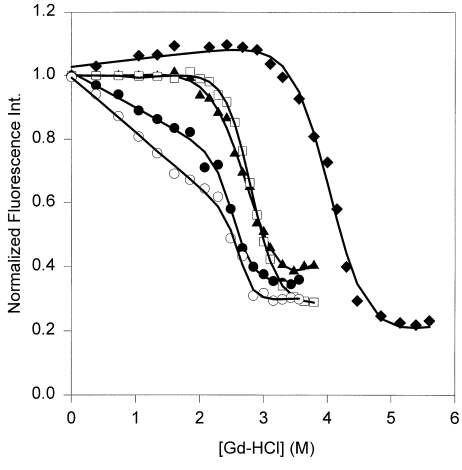

Fig. 3. Changes of fluorescence intensity during chemical denaturation of terbium-loaded F102W excited at 295 nm (Trp emission) (●), F102W excited at 285 nm (Tb^{3+} emission) (○), Y65W (▲), Y57W (□) and CDOM33 (♦). The symbols are the experimentally derived data points. The solid lines are the lines-of-best-fit as determined by fitting to Eq. (1). Fitting parameters are given in Table 3.

Upon binding of Tb^{3+}, the stability of Y57W increased by 17%, showing that the changes in the conformation of the loop upon binding of Tb^{3+} were significant. Terbium-loaded CDOM33 showed an enhancement in free energy (23%) which was slightly larger than that observed for Y57W, and a substantial enhancement of $C_{1/2}$ (from 2.2 M to 4.1 M) compared to Y57W. This behaviour was not unexpected since the binding affinity of the modified CD loop is about ten times higher than the original CD loop [20]. For Y65W the free energy did not change upon binding of Tb^{3+}. However, the transition midpoint increased by 43% compared to Ca^{2+}-loaded protein.

For F102W both the Trp and terbium signal decreased steadily by about 25–30% before unfolding started at about 2.0 M GdHCl, and then decreased sharply by about 40% during the unfolding process until unfolding finished at about 3.0 M GdHCl. The data in Table 3 indicate that the free energy and denaturant index both increased slightly when Tb^{3+} luminescence was monitored instead of Trp fluorescence. However, the $C_{1/2}$ value was identical in both cases. These results suggested that both the F-helix and the loop regions unfolded at the same time, as reported earlier. The free energy of the unfolding process of F102W in the presence of Tb^{3+} was 54% greater than was obtained in the presence of Ca^{2+}. Furthermore, the $C_{1/2}$ value increased by ca. 44%, which was in reasonable agreement with the changes in $C_{1/2}$ for Y57W.

It is noteworthy that the $C_{1/2}$ and free energy values of the terbium-loaded proteins all increased compared to Ca^{2+}-loaded or apo proteins no matter where the Trp was located. For example, all apo OM proteins had ΔG_{un} values lower than 4.0 kcal mol^{-1}. ΔG_{un} values of calcium-loaded proteins increased to 5.3–7.4 kcal mol^{-1} and ΔG_{un} values of terbium-loaded proteins were 6.7–8.5 kcal mol^{-1} (with the exception of F102W monitored by Tb^{3+} lumines-

cence, which was 11.1 kcal mol^{-1}). Hence, as the binding affinity increases, the stability of the protein increases, and reaches what appears to be a limiting value in the region of 8–9 kcal mol^{-1}. The results also show that the more tightly bound Tb^{3+} ion fully overcomes the destabilization which appears to occur upon insertion of a Trp into position 102. It is possible that the higher valence of Tb^{3+} may increase the number of oxygen donor groups from the protein bound to the metal, thus increasing the stability of the protein–metal complex.

3.5. Thermal denaturation of Ca^{2+}-free proteins

The spectral characteristics of apo OM proteins during thermal denaturation are shown in Table 4. As was the case for chemical denaturation, all spectra showed a substantial red-shift and an increase of FWHM during unfolding. The thermal unfolding curves for apo proteins are shown in Fig. 4. In all cases, the unfolding process started at a relatively low temperature, and unfolding was completed within a relatively narrow temperature range. Thermally induced unfolding profiles were analyzed by fitting the unfolding curve to Eqs. (2) and (3), and the results are given in Table 5. Calculation of the ΔG_{un} value required that the temperature dependence of

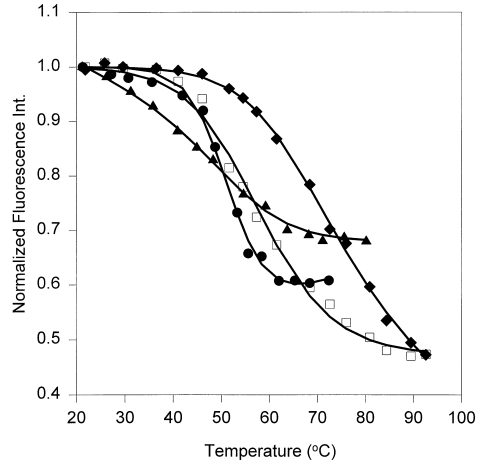

Fig. 4. Changes of fluorescence intensity as a function of temperature for calcium-free oncomodulin mutants. F102W (●), Y65W (▲), Y57W (□) and CDOM33 (♦). The symbols are the experimentally derived data points. The solid lines are the lines-of-best-fit as determined by fitting to Eq. (2). Fitting parameters are given in Table 5.

Table 4
Changes in fluorescence properties of apo and Ca^{2+}-loaded oncomodulin mutants during thermal denaturation

Proteins	Change in intensity (Trp)[a]	Change in FWHM (nm)	Change in λ_{max} (nm)
Y57W			
Ca^{2+}-free	47% decrease	55–60–57[b]	339–345–339[c]
Ca^{2+}-loaded	17% decrease	53–59–55	339–345–339
Tb^{3+}-loaded	20% increase	53–60–54	339–345–339
Y65W			
Ca^{2+}-free	33% decrease	55–57–55	343–345–343
Ca^{2+}-loaded	36% decrease	55–57–55	343–345–343
Tb^{3+}-loaded	20% decrease	55–57–56	343–345–343
F102W			
Ca^{2+}-free	40% decrease	47–64–51	316–345–316
Ca^{2+}-loaded	72% decrease	39–64–40	315–345–315
Tb^{3+}-loaded	80% decrease	39–63–41	315–345–316
CDOM33			
Ca^{2+}-free	47% decrease	54–58–56	339–345–339
Ca^{2+}-loaded	61% decrease	53–59–53	339–343–339
Tb^{3+}-loaded	58% decrease	53–59–54	339–343–340

[a] Data were corrected by the thermal quenching curve of Lys–Trp–Lys.
[b] Data represented FWHM of native protein, denatured protein and recovered protein.
[c] Data represent λ_{max} values of native, denatured and recovered protein, respectively.

Table 5
Enthalpy changes for thermal unfolding of oncomodulin mutants

Proteins	ΔH^0_{un} (kcal mol^{-1})	ΔS^0_{un} (cal mol^{-1} K^{-1})	T_{un} (°C)	ΔG_{un} (20°C)[e] (kcal mol^{-1})
Ca^{2+}-free[a]				
Y57W	28.0 ± 4.4	85.0 ± 6.0	55.9 ± 0.5	2.4 ± 0.3
Y65W	19.4 ± 2.0	59.4 ± 4.8	52.8 ± 0.4	1.4 ± 0.2
F102W	54.0 ± 6.2	166.6 ± 5.9	50.9 ± 0.4	4.6 ± 0.5
CDOM33	28.8 ± 2.7	83.9 ± 4.1	70.1 ± 0.5	3.0 ± 0.3
Ca^{2+}-loaded[b]				
Y57W	28.4 ± 3.1	82.8 ± 8.7	70.0 ± 0.5	3.0 ± 0.4
Y65W	23.9 ± 2.5	72.1 ± 5.6	58.0 ± 0.4	2.0 ± 0.3
F102W	89.7 ± 9.1	258.8 ± 11.4	73.8 ± 0.3	12.5 ± 1.2
CDOM33	76.9 ± 7.8	218.4 ± 10.5	79.1 ± 0.3	11.2 ± 1.2
Tb^{3+}-loaded[c]				
Y57W[d]	67.5 ± 7.5	190.6 ± 12.8	81.7 ± 0.4	9.9 ± 1.0
Y65W	61.7 ± 6.6	184.2 ± 11.9	61.6 ± 0.4	6.8 ± 0.7
F102W	74.4 ± 8.3	207.6 ± 15.1	86.4 ± 0.4	11.6 ± 1.1
CDOM33[d]	91.1 ± 9.6	252.6 ± 10.9	87.7 ± 0.4	14.9 ± 1.7

[a] Fitting parameters for apo proteins were as follows: F102W: $F_{0N} = 1.011$, $F_{0U} = 0.721$, $s_N = -0.012$, $s_U = -0.007$; Y65W: $F_{0N} = 0.998$, $F_{0U} = 0.669$, $s_N = -0.004$, $s_U = -0.006$; Y57W: $F_{0\ N} = 0.997$, $F_{0U} = 0.821$, $s_N = -0.010$, $s_U = -0.008$; CDOM33: $F_{0N} = 1.001$, $F_{0U} = 0.724$, $s_N = -0.009$, $s_U = -0.006$.
[b] Fitting parameters for Ca^{2+}-loaded proteins were as follows: F102W: $F_{0N} = 1.005$, $F_{0U} = 0.301$, $s_N = 0.009$, $s_U = 0.002$; Y65W: $F_{0N} = 0.999$, $F_{0U} = 0.470$, $s_N = -0.008$, $s_U = -0.004$; Y57W: $F_{0N} = 1.001$, $F_{0U} = 0.922$, $s_N = -0.013$, $s_U = -0.007$; CDOM33: $F_{0N} = 1.034$, $F_{0U} = 0.484$, $s_N = -0.009$, $s_U = -0.003$.
[c] Fitting parameters for Tb^{3+}-loaded proteins were as follows: F102W: $F_{0N} = 1.030$, $F_{0U} = 0.160$, $s_N = -0.009$, $s_U = 0.000$; Y65W: $F_{0N} = 1.009$, $F_{0U} = 0.076$, $s_N = -0.014$, $s_U = 0.002$; Y57W: $F_{0N} = 1.002$, $F_{0U} = 0.086$, $s_N = 0.040$, $s_U = 0.000$; CDOM33: $F_{0N} = 1.012$, $F_{0U} = 0.280$, $s_N = -0.008$, $s_U = -0.000$.
[d] The thermodynamic parameters were obtained by fitting Tb^{3+} luminescence data.
[e] Free energy values were calculated using Eq. (3) with $\Delta C_{p,un} = 1330$ (cal mol^{-1} K^{-1}) for the apo form and 1100 (cal mol^{-1} K^{-1}) for the Ca^{2+}- and Tb^{3+}-loaded forms [16], with a reference temperature of 293 K.

ΔH_{un} and ΔS_{un} be accounted for by including a term for the differential heat capacity of the folded and unfolded protein ($\Delta C_{p,un}$). The value we used was 1330 cal (deg mol)$^{-1}$ for the apo form, and 1100 cal (deg mol)$^{-1}$ for the Ca^{2+}- and Tb^{3+}-loaded forms [16].

The results showed that the thermal stability of the apo proteins was quite low. For single-Trp OM mutants the transition midpoint (T_{un}) values were very close (within 5°C of each other). The free energy values showed that, when compared to Y57W, the apo-form of Y65W was less stable whereas the apo-CDOM33 mutant was more stable. This trend was in agreement with that found during chemical denaturation of the apo mutants. Interestingly, the F102W mutant had the highest free energy among these proteins even though the T_{un} value was the lowest of the four proteins studied. This correlates to the increased values of both the enthalpy and entropy terms. Given that the apo form of the F102W mutant showed very poor stability towards chemical denaturation, it is possible that the increased free energy is the result of incomplete removal of the Ca^{2+} from the protein. It is also possible that GdHCl is better able to denature proteins compared to thermal denaturation methods, possibly due to electrostatic interactions between the positively charged denaturant and the protein, which has a net charge of −15 at neutral pH [34].

CDOM33 had the highest transition midpoint (over 15°C higher than the other mutants) and a slightly lower free energy value than F102W (about 0.9 kcal mol^{-1} lower). These results may reflect slight differences in the stability imparted by the novel CD loop structure as compared to the native CD loop of the other proteins.

3.6. Thermal denaturation of Ca^{2+}-loaded proteins

The spectral characteristics of holo OM mutants during thermal denaturation are shown in Table 4 and the unfolding curves are shown in Fig. 5. The results of the thermodynamic analysis of the unfolding curves is given in Table 5. In all cases, denaturation caused a decrease in the fluorescence intensity, a red shift in the emission maximum and an increase in the FWHM. The unfolding curves were significantly different than those obtained from chemical denaturation, mainly owing to the additional contribution from thermally induced quenching of fluorescence. The holo form of the proteins had T_{un} values which were higher than the values obtained for the apo form, consistent with binding of the metal ions to the folded state of the protein. Interestingly, the thermal denaturation profiles of the holo-oncomodulin mutants showed a different trend compared to the chemical denaturation profiles. Binding of Ca^{2+} caused the unfolding temperature of Y57W to increase by 14°C while the free energy of unfolding increased by 1.2 kcal mol^{-1}. The Y65W protein showed smaller Ca^{2+}-dependent increases in local unfolding temperature and free energy, in agreement with the results from chemical denaturation.

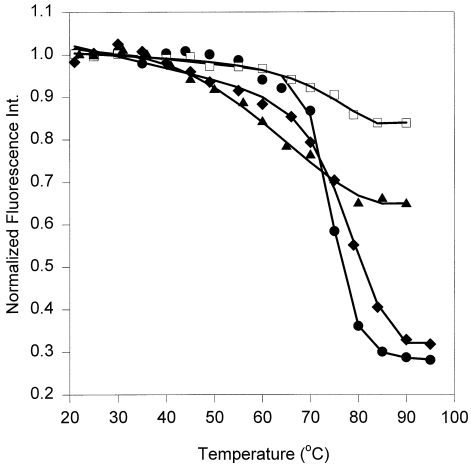

Fig. 5. Changes of fluorescence intensity during thermal denaturation of calcium-loaded F102W (●), Y65W (▲), Y57W (□) and CDOM33 (♦). The symbols are the experimentally derived data points. The solid lines are the lines-of-best-fit as determined by fitting to Eq. (2). Fitting parameters are given in Table 5.

F102W showed a significant increase in both the unfolding midpoint (73.8°C) and the free energy of thermal unfolding upon binding of Ca^{2+}, suggesting that the binding of Ca^{2+} is fundamentally important in stabilizing the F-helix against the hydrophobic core. Perhaps most important is the significant increase in both the local enthalpy and entropy of unfolding as probed by Trp-102 on going from the apo to the holo forms. Neither Y57W nor Y65W show such large increases. This is consistent with destabilization of the apo form of the protein when Trp is located at position 102, in agreement with the chemical denaturation results. Once again, the F102W protein showed lower stability for chemical denaturation as compared to thermal denaturation, supporting the suggestion that electrostatic interactions between GdHCl and the protein may have affected the unfolding behaviour.

In the case of the CDOM33 there was also a large increase in thermal stability upon binding of Ca^{2+}. Both the enthalpy and entropy of the unfolding transition increased dramatically, resulting in an increase in both the unfolding transition temperature and the free energy of unfolding. These results agreed with the results from the chemical stability studies which showed that altering the binding affinity of the loop improved the stability of calcium binding proteins. The large increase in enthalpy and entropy for CDOM33 compared to Y57W is most likely due to the differences in the mode of binding to metal ions in the two loops. For Y57W, there is a bridging water in the binding loop at Asp-59 which participates in the binding process. For CDOM33, the Glu-59 residue participates directly in coordinating to the bound metal ion without the bridging water. The entropy and enthalpy of the nearby Trp residue would be expected to change dramatically upon binding of metal ions. The direct coordination without the need for bridging water molecules may also explain the much higher overall stability of CDOM33 during both chemical and thermal denaturation.

The free energy and unfolding temperature values obtained for Ca^{2+}-loaded OM mutants were in all cases lower than the values obtained by Henzl and co-workers [16] for native rat oncomodulin and various mutants with Ca^{2+} bound. This discrepancy is likely due to the lower ionic strength used in our work (100 mM KCl) as compared to the work by

Henzl and coworkers (150 mM NaCl). The stability of oncomodulin has been reported to be highly dependent on the level of salt present, owing to electrostatic contributions to the conformational stability of the protein [35].

3.7. Thermal denaturation of Tb^{3+}-loaded proteins

Binding of terbium instead of calcium also improved the thermal stability of each protein studied. The thermal unfolding curves of terbium-loaded proteins are shown in Fig. 6, while the thermodynamic data is given in Table 5. The unfolding curves for Y57W and CDOM33 mutants were obtained from changes in Tb^{3+} luminescence, while the unfolding curves for Y65W and F102W were obtained from changes in the intensity of Trp fluorescence. Interestingly, the transition midpoints and free energy of unfolding for Y57W increased significantly compared to the case where Ca^{2+} was bound. This is further supported by the large increases in the enthalpy and entropy of unfolding on going from Ca^{2+} to Tb^{3+}. The enthalpy, entropy and free energy of the Y65W also increased substantially upon binding of Tb^{3+}, suggesting that there was a major conformational change in the protein upon binding of the more highly charged lanthanide ion, in agreement with the chemical denaturation results. Interestingly, the free energy of terbium-loaded F102W appeared to be lower than calcium-loaded protein even though the T_{un} value was improved. However, the standard deviation in the enthalpy and entropy values was quite large since the unfolding curve showed no post-unfolding region owing to the upper temperature limit of our instrument (95°C), which was past the point where unfolding was completed. Hence, it is possible that there was not a significant difference in stability upon binding of Tb^{3+}. For CDOM33, the binding of Tb^{3+} increased all thermodynamic values. This is consistent with the higher coordination number for Tb^{3+} as compared to Ca^{2+}, and is in agreement with the chemical denaturation studies.

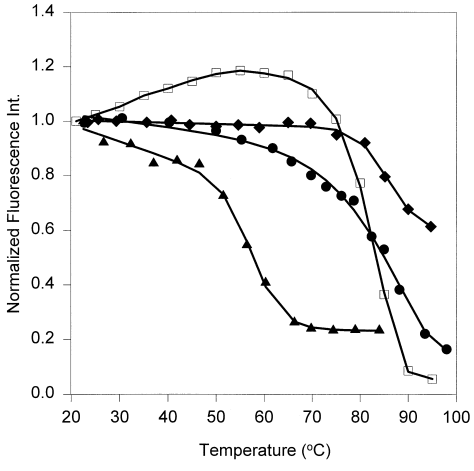

Fig. 6. Fluorescence intensity changes during thermal denaturation of terbium-loaded F102W (●), Y65W (▲), Y57W (□) and CDOM33 (♦). The symbols are the experimentally derived data points. The solid lines are the lines-of-best-fit as determined by fitting to Eq. (2). Fitting parameters are given in Table 5.

4. Conclusions

This study has shown that single Trp mutants of the Ca^{2+}-binding protein oncomodulin can provide useful information on effects of point mutations on the stability of the protein when different levels or types of metal ions are bound. In all cases, the binding of metal ions resulted in large improvements in both the chemical and thermal stability of the protein. Comparison of the stability of proteins upon binding of different ions showed clearly that both thermal and chemical stability were improved upon binding of metal ions with the order apo $< Ca^{2+} <$ Tb^{3+}. The thermodynamic parameters obtained in this work reflect global denaturation of protein structure reported from different locations. The thermodynamic values provided information on the degree to which the presence of the Trp at different locations either stabilized or destabilized the folding of the protein, and how the presence of different metal ions influenced this effect. Overall, the results suggested that increasing the number of metal ligating oxygens in the binding site, either by using a metal ion with a higher coordinate number (i.e., Tb^{3+}) thereby drawing in more carboxylate ligands, or by providing more ligating groups, as in the CDOM33 replacement, produces notable improvements in protein stability. This strongly suggests that the metal ion must be removed before protein unfolding occurs.

Acknowledgements

The authors thank the Natural Sciences and Engineering Research Council of Canada for funding this work. We also thank Professor Arthur G. Szabo for donating the protein samples and for providing access to fluorescence lifetime instrumentation.

References

[1] R.D. Kidd, H.P. Yennawar, P. Sears, C. Wong, G.K. Farber, J. Am. Chem. Soc. 118 (1996) 1645.
[2] O. Farver, L.K. Skov, S. Young, N. Bonander, B.G. Karlsson, T. Vanngard, I. Pecht, J. Am. Chem. Soc. 119 (1997) 5453.
[3] Y. Blancuzzi, A. Padilla, J. Parallo, A. Cave, Biochemistry 32 (1993) 1302.
[4] H.H. Bauer, M. Müller, J. Goette, H.P. Merkle, U.P. Fringeli, Biochemistry 33 (1994) 1227.
[5] R. Roskoski, L.G. Gahn, Biochemistry 34 (1995) 252.
[6] A.M. Beasty, M. Hurle, J.T. Manz, T. Stackhouse, C.R. Mathews, in: D.L. Oxender (Ed.), Protein Structure, Folding and Design, Alan R. Liss, New York, 1986, p. 259.
[7] M.R. Eftink, Biophy. J. 66 (1994) 482.
[8] J.M. Sanz, A.R. Fersht, FEBS Lett. 344 (1994) 216.
[9] N.S. Sampson, I.J. Kass, J. Am. Chem. Soc. 119 (1997) 855.
[10] K. Sudhakar, C.M. Philips, C.S. Owen, J.M. Vanderkooi, Biochemistry 34 (1995) 1355.
[11] M. Laberge, W.W. Wright, K. Sudhakar, P.A. Liebman, J.M. Vanderkooi, Biochemistry 36 (1997) 5363.
[12] J.P. MacManus, Cancer Res. 39 (1979) 3000.
[13] D. Bernaert, L.M. Brewer, J.P. MacManus, P. Galand, Int. J. Cancer. 43 (1989) 719.
[14] J.P. MacManus, L.M. Brewer, M. Yaguchi, Eur. J. Biochem. 136 (1983) 9.
[15] W.C. Barker, L.K. Ketcham, M.D. Dayhoff, in: M.D. Dayhoff (Ed.), Atlas of Protein Sequences and Structure, 1978, p. 273.
[16] M.T. Henzl, R.C. Hapak, E.A. Goodpasture, Biochemistry 35 (1996) 5856.
[17] J.A. Cox, M. Milos, J.P. MacManus, J. Biol. Chem. 265 (1990) 6633.
[18] J.P. MacManus, A.G. Szabo, R.E. Williams, Biochem. J. 220 (1984) 261.
[19] C.M.L. Hutnik, J.P. MacManus, D. Banville, A.G. Szabo, Biochemistry 30 (1991) 7652.
[20] I.D. Clark, A.J. Bruckman, C.W.V. Hogue, J.P. MacManus, A.G. Szabo, J. Fluorescence 4 (1994) 235.
[21] C.M.L. Hutnik, J.P. MacManus, D. Banville, A.G. Szabo, J. Biol. Chem. 265 (1990) 11456.
[22] C.M.L. Hutnik, J.P. MacManus, A.G. Szabo, Biochemistry 29 (1990) 7318.
[23] C.W.V. Hogue, J.P. MacManus, D. Banville, A.G. Szabo, J. Biol. Chem. 267 (1992) 13340.
[24] D.L. Dexter, J. Chem. Phys. 21 (1953) 836.
[25] J.P. MacManus, C.M.L. Hutnik, B.D. Sykes, A.G. Szabo, T.C. Williams, D. Banville, J. Biol. Chem. 264 (1988) 3470.
[26] T.D. Barela and, A.D. Sherry, Anal. Biochem. 71 (1976) 351.
[27] L. Zheng, W.R. Reid, J.D. Brennan, Anal. Chem. 69 (1997) 3940.
[28] M.M. Santoro, D.W. Bolen, Biochemistry 27 (1988) 8063.
[29] E.P. Kirby, R.F. Steiner, J. Phys. Chem. 74 (1970) 4480.
[30a] M.R. Eftink, C.A. Ghiron, Biochemistry 16 (1977) 5546.
[30b] M.R. Eftink, C.A. Ghiron, J. Phys. Chem. 5 (1977) 486.
[31a] C.M.L. Hutnik, A.G. Szabo, Biochemistry 28 (1989) 3923.
[31b] K.J. Willis, A.G. Szabo, Biochemistry 28 (1989) 4902.
[32] F.R. Ahmed, M. Przybylska, D.R. Rose, G.I. Birnbaum, M.E. Pippy, J.P. MacManus, J. Mol. Biol. 216 (1990) 127.
[33] M. She, W.-J. Dong, P.K. Umeda, H.C. Cheung, Biophys. J. 73 (1997) 1042.
[34] M.F. Gillen, D. Banville, R.G. Rutledge, S. Narang, V.L. Seligy, J.F. Whitfield, J.P. MacManus, J. Biol. Chem. 262 (1987) 5308.
[35] V.V. Filimonow, W. Pfeil, T.N. Tsalkova, P.L. Privalov, Biophys. Chem. 8 (1978) 117.